

Mutational and functional analysis of *N*-linked glycosylation of envelope fusion protein F of *Helicoverpa armigera* nucleopolyhedrovirus

Shu Shen,¹ Manli Wang,¹ Xin Li,^{1,2} Shufen Li,¹ Monique M. van Oers,³ Just M. Vlask,³ Ineke Braakman,² Zhihong Hu,¹ Fei Deng¹ and Hualin Wang¹

Correspondence

Hualin Wang
h.wang@wh.iov.cn
Fei Deng
df@wh.iov.cn

¹State Key Laboratory of Virology, and Joint Laboratory of Invertebrate Virology, Wuhan Institute of Virology, Chinese Academy of Sciences, Wuhan 430071, PR China

²Cellular Protein Chemistry, Bijvoet Center for Biomolecular Research, Utrecht University, The Netherlands

³Laboratory of Virology, Wageningen University, The Netherlands

The envelope fusion (F) protein of baculoviruses is a heavily *N*-glycosylated protein that plays a significant role in the virus infection cycle. *N*-Linked glycosylation of virus envelope glycoprotein is important for virus envelope glycoprotein folding and its function in general. There are six predicted *N*-glycosylation sites in the F (HaF) protein of *Helicoverpa armigera* nucleopolyhedrovirus (HearNPV). The *N*-glycosylation site located in the F₂ subunit (N104) of HaF has been identified and functionally characterized previously (Long *et al.*, 2007). In this study, the other five potential *N*-glycosylation sites located in the HaF₁ subunit, namely, N293, N361, N526, N571 and N595, were analysed extensively to examine their *N*-glycosylation and relative importance to the function of HaF. The results showed that four of these five potential glycosylation sites in the F₁ subunit, N293, N361, N526 and N571, were *N*-glycosylated in F proteins of mature HearNPV budded viruses (BVs) but that N595 was not. In general, the conserved site N526 was critical to the functioning of HaF, as absence of *N*-glycosylation of N526 reduced the efficiency of HaF folding and trafficking, consequently decreased fusogenicity and modified the subcellular localization of HaF proteins, and thus impaired virus production and infectivity. The absence of *N*-glycosylation at other individual sites was found to have different effects on the fusogenicity and subcellular distribution of HaF proteins in HzAM1 cells. In summary, *N*-glycosylation plays comprehensive roles in HaF function and virus infectivity, which is further discussed.

Received 20 November 2015

Accepted 13 January 2016

INTRODUCTION

N-Linked glycans play a key role in directing proper folding, stability, intracellular trafficking and fusogenic activity of viral glycoproteins, which directly correlate with virus morphogenesis and infectivity. Many viral proteins are modified by the host cellular glycosylation machinery in order to ensure proper function and virus–host interactions. *N*-Glycosylations of various viral envelope proteins have been studied in much detail. For example, *N*-glycosylation of the haemagglutinin (HA) of influenza virus is important in modulating protein maturation and folding (Danielsson *et al.*, 2003), fusion activity (Ohuchi *et al.*, 1997b) and receptor affinity (Ohuchi *et al.*, 1997a), as well as antigenicity (Abe *et al.*, 2004).

The *N*-glycosylation site occupancies have an influence on the structure and function of glycoproteins (Jones *et al.*, 2005). In the *N*-glycosylation process, the *N*-glycosylation sequence (N-X-S/T) of glycoproteins, normally called the *N*-glycosylation sequon, is necessary for the recognition of the oligosaccharide transferase complex and the transfer of oligosaccharides onto the conserved asparagine (N) of the sequon. Once the sequon is disrupted, *N*-glycosylation would be abolished, which may affect the glycoprotein structure and function.

In members of the family *Baculoviridae*, the envelope fusion protein (EFP) is the major glycoprotein present in the envelopes of budded virus (BV). So far, two different types of EFP, GP64 and the F protein, have been identified. GP64s are class III EFPs and are identified only in members of group I of the genus *Alphabaculovirus* (Kadlec *et al.*, 2008). F proteins, assumed to be the ancestral EFPs of

One supplementary table and two figures are available with the online Supplementary Material.

baculoviruses, are widely found in members of the genera *Betabaculovirus* and *Deltabaculovirus* and group II of the genus *Alphabaculovirus* (Pearson *et al.*, 2000). The F protein possesses the common features of class I EFPs. The precursor F₀ is synthesized in the endoplasmic reticulum (ER) and undergoes proteolytic cleavage by the *trans*-Golgi network protease furin (IJkel *et al.*, 2000). The two resulting subunits (F₁ and F₂) are linked by disulfide bonds (Long *et al.*, 2006). Mature F protein is subsequently transported to the plasma membrane and finally incorporated into the viral envelope during BV budding. During the BV entry process, F proteins bind to an elusive cellular receptor and mediate fusion between the viral envelope and the endosome membrane to release viral nucleocapsids for replication (Tan *et al.*, 2008; Westenberg *et al.*, 2004). Therefore, efficient receptor binding, membrane fusion and virus egress depend largely on the proper functioning of the F protein.

The F protein (HaF) of *Helicoverpa armigera* nucleopolyhedrovirus (HearNPV) contains six predicted N-glycosylation sequons (N-X-S/T), five in the F₁ subunit and one in the F₂ subunit. Deglycosylation assays have demonstrated that both the F₁ and F₂ subunits of HaF are N-glycosylated (Long *et al.*, 2006). The unique N-glycosylation site in F₂ located at site N104 has been found to be important for virus infectivity (Long *et al.*, 2007). The functions and significance of the remaining five potential sites, N293, N361, N526, N571 and N595, located in the F₁ subunit, have not been analysed so far. As N-glycosylation is a prerequisite for correct folding and functioning of the viral glycoprotein, a further in-depth study on the N-glycosylation of HaF is important to better understand its significance in the function of baculovirus F proteins. In this study, a series of single mutation at each putative site of HaF were introduced, and recombinant HearNPVs harbouring the various mutated HaFs were constructed. The mutant viruses were tested for N-glycosylation, fusogenicity and intracellular trafficking of the F proteins, as well as for virus replication and BV production.

RESULTS

Identification of N-glycosylation sites in the F₁ subunit of HaF by site-directed mutagenesis

HaF contains six predicted N-glycosylation site consensus sequons (N-X-S/T), comprising N104 in the F₂ subunit and N293, N361, N526, N571 and N595 in the F₁ subunit. N293, N526 and N571 are more conserved among the baculovirus F homologues than N104, N361 and N595 (Fig. 1a). N104 has been identified as the sole N-glycosylation site in the HaF₂ subunit (Long *et al.*, 2007). In this research, six mutant viruses carrying single-site mutations – F^{N104Q}, F^{N293S}, F^{N361Q}, F^{N526S}, F^{N571S} and F^{N595S} – were generated to abolish each N-glycosylation site, respectively (Fig. 1b). Transfection and infection assays showed that all of these ‘single-site’ mutants produced foci of transfected

cells indicating viable virus production and spread (Fig. 1c, upper panels) and that supernatants of these transfected cells were able to infect healthy cells (Fig. 1c, lower panels), although with different efficiencies of EGFP expression. This also indicated that absence of potential N-glycosylation at these positions individually did not abort HearNPV infectivity.

Western blot analysis was performed to identify a possible shift in molecular masses of the various HaF mutant proteins as a consequence of the mutations in both BVs (Fig. 2a) and infected cells (Fig. 2b). As a positive control, WT HaF was efficiently processed into F₁ and F₂ subunits, retaining only a small amount of uncleaved F₀ (Fig. 2, lanes a1, a6 and a11, and lane b5). Consistent with a previous report (Long *et al.*, 2007), the results confirmed that N104 in the F₂ subunit is N-glycosylated (Fig. 2, lanes a8 and b9). A slightly faster-migrating F₁ band was detected in F^{N293S}, F^{N361Q}, F^{N526S} and F^{N571S} (Fig. 2, lanes a2–a5 and b1–b4), suggesting that the N-X-S/T sequons at these four sites were utilized for glycosylation. In contrast, both F₂ and F₁ bands of F^{N595S} (Fig. 2, lanes a9 and b7) in BVs and infected cells appeared similar to the WT HaF (Fig. 2, lanes a11 and b5), suggesting N595 is not used for N-glycosylation in the F₁ subunit. The Western blot results further suggested that all the single mutations seemed to have little impact on the expression levels of HaF (Fig. 2b) and the incorporation of F proteins into BVs (Fig. 2a).

Rescue assay of N-glycosylation by nearby generated N-glycosylation sequons

To investigate whether the N-glycosylation site occupancy in HaF is a specific process, F^{N104S} and F^{N361S} mutants were also generated (Fig. 1b). These two mutants were different from F^{N104Q} and F^{N361Q} in that they not only abolished the native sites at N104 and N361 but at the same time created two new N-glycosylation sequons nearby, N-K-S at N102 and N-N-S at N359, respectively. The results of Western blotting showed that the molecular masses of the F^{N361S} subunits (Fig. 2, lanes a10 and b6) appeared to be equivalent to the WT HaF (Fig. 2, lanes a11 and b5), suggesting that the N-glycosylation was probably rescued in F^{N361S}. The newly created glycosylation site at N102 could not fully rescue N-glycosylation of F₂ subunit in the BV and cell samples. The F₂ subunits of a small portion of F^{N104S} proteins were glycosylated, as most of the F^{N104S} F₂ subunit sample ran faster, leaving a very weak signal of glycosylated F₂ with a similar molecular mass to the WT HaF₂ (Fig. 2, lanes a7 and b8, arrowheads). Therefore, N104 may be a specific N-glycosylation site in the F₂ subunit that plays an irreplaceable role in HaF functions.

Impact of elimination of individual N-glycosylation sites on infectious BV production and virus infectivity

The *in vitro* growth properties of the various mutant viruses were investigated (Fig. S1, available in the online

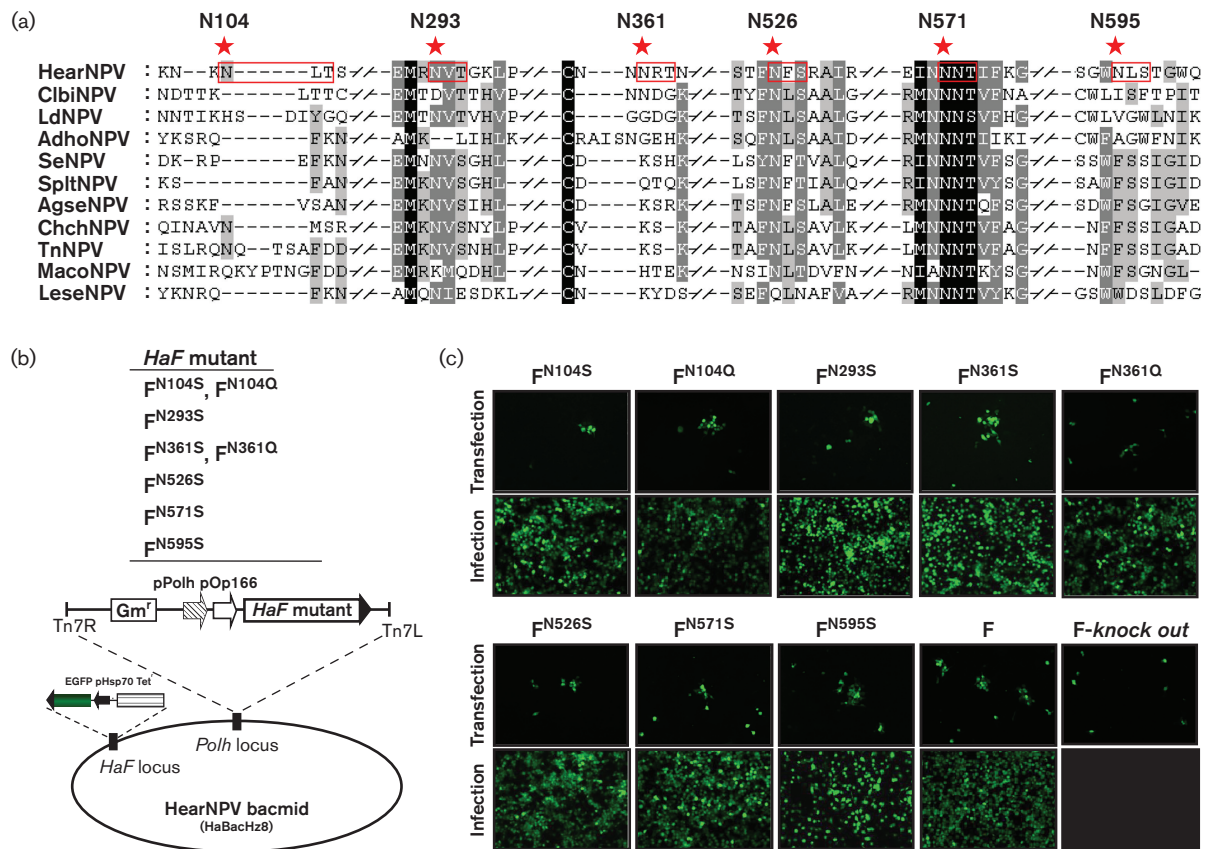


Fig. 1. Construction of mutant viruses carrying F proteins with mutations at putative *N*-glycosylation sites. (a) Sequence comparison of F proteins from members of group II nucleopolyhedroviruses (NPVs). The putative *N*-glycosylation sequons of HearNPV F protein are boxed in red colour, with asparagines (N) for oligosaccharide attachment indicated by asterisks. Conserved asparagines are shown in white characters on a black or grey background. The GenBank accession numbers of these virus F proteins and virus full names are as follows: NP_075202 (*Helicoverpa armigera* NPV, HearNPV), YP_717667 (*Clanis bilineata* NPV, ClibiNPV), NP_047767 (*Lymantria dispar* NPV, LdNPV), NP_818765 (*Adoxophyes honmai* NPV, AdhoNPV), NP_037768 (*Spodoptera exigua* NPV, SeNPV), YP_002332708 (*Spodoptera litura* NPV, SpItNPV), YP_529678 (*Agrotis segetum* NPV, AgseNPV), YP_249754 (*Chrysodeixis chalcites* NPV, ChchNPV), YP_309032 (*Trichoplusia ni* single NPV, TnNPV), NP_689183 (*Mamestra configurata* NPV, MacoNPV) and YP_758463 (*Leucania separata* NPV, LeseNPV). (b) Schematic representation of mutant *f*-null HearNPV bacmids with various mutations at putative *N*-glycosylation sites in the *f* gene, including eight mutant bacmids with single mutations. The mutated sites involved for each single-site mutant bacmid are in superscript. pOp166, 166 bp *Orgyia pseudotsugata* multicapsid NPV fusion protein (ORF126) promoter; pPolh, *Autographa californica* multicapsid NPV polyhedrin promoter; Tn7R and Tn7L, the right and left insertion sites, respectively, of mini-AttTn7; Gm^r, gentamicin resistance gene; Tet^r, tetracycline resistance genes. (c) Transfection and infection assay. HzAM1 cells were transfected with each mutant bacmid. *f*-null and *f*-rescued HearNPV bacmids were used as controls. The cells were monitored by fluorescence microscopy at 72 h post-transfection and 96 h post-infection.

Supplementary Material). We found that mutant viruses carrying F^{N526S} ($2.2 \times 10^5 \pm 1.2 \times 10^5$ TCID₅₀ ml⁻¹, mean \pm SD) yielded much less infectious BVs than the control virus ($4.0 \times 10^6 \pm 2.1 \times 10^6$ TCID₅₀ ml⁻¹) ($P < 0.01$) (Fig. 3a). Infectious BVs of F^{N526S} could barely be detected at 24 h post-infection (p.i.), and the BV titre of F^{N526S} was more than 10 times lower than that of the control virus ($P < 0.01$) (Fig. S1 and Table 1). These indicated that F^{N526S} was the most severely impaired among all the mutant viruses. BV production of F^{N104Q}, F^{N293S} and F^{N571S} was about 5–10 times lower than that of the control

($P < 0.05$) (Fig. 3a). F^{N595S} ($2.0 \times 10^6 \pm 1.8 \times 10^6$ TCID₅₀ ml⁻¹) showed similar BV production levels to the WT control ($P > 0.05$) (Fig. 3a). F^{N361Q} ($2.0 \times 10^6 \pm 0.0 \times 10^6$ TCID₅₀ ml⁻¹) also produced infectious BVs at 72 h p.i. of similar titres to the control virus (Fig. 3a), suggesting that *N*-glycosylation of N361 makes little contribution to virus production. However, one of the *N*-glycosylation-site-rescued HaF mutants, F^{N361S}, yielded BV levels ($1.0 \times 10^6 \pm 0.7 \times 10^6$ TCID₅₀ ml⁻¹) about four times less than the control ($P < 0.05$), suggesting that it could not fully rescue the BV titres although *N*-glycosylation of

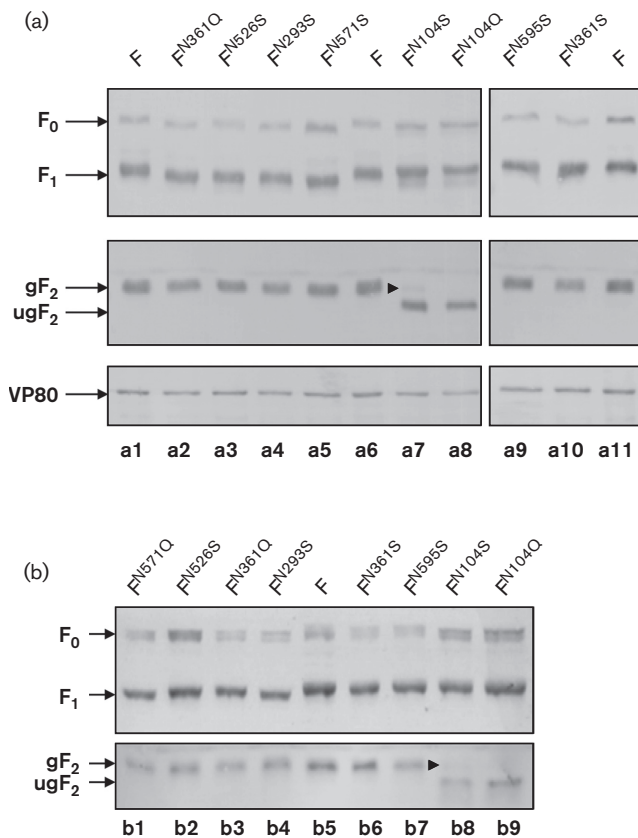


Fig. 2. Western blot analysis of WT and mutant HearNPV F protein incorporation in BVs and expression in infected HzAM1 cells. (a) F₁ and F₂ were detected in purified BVs by Western blotting (top and middle panels). VP80 was detected as an internal control (bottom panel). (b) F protein expression in infected HzAM1 cells was analysed by Western blotting. a1, a6, a11 and b5, WT F; a2 and b3, F^{N361Q}; a3 and b2, F^{N526S}; a4 and b4, F^{N293S}; a5 and b1, F^{N571S}; a7 and b8, F^{N104S}; a8 and b9, F^{N104Q}; a9 and b7, F^{N595S}; a10 and b6, F^{N361S}. g, Glycosylated; ug, unglycosylated.

HaF might be rescued at N359 (Fig. 3b and S1). Therefore, the N-glycosylation of N361 site may not be critical for virus properties, and the compensation of N-glycans at neighbouring positions (N359) may be redundant and unnecessary. The titre of the other site-rescued mutant F^{N104S} ($3.4 \times 10^5 \pm 2.4 \times 10^5$ TCID₅₀ ml⁻¹) was about 10 times lower than that of the control (Fig. 3b) ($P < 0.01$). As F^{N104S} could not fully rescue N-glycosylation of HaF and the BVs titre of F^{N104S} was similar to F^{N104Q} in the absence of N-glycans in F₂ subunit, this indicated that N-glycosylation of the HaF₂ subunit is important for virus production.

The infectivity of the mutant baculoviruses at 96 h p.i. was also determined as genomic DNA copies per TCID₅₀ (Table 1). For the control virus (vHaBacΔF-HaF), 1 TCID₅₀ was equivalent to approximately 10^4 copies of viral genomic DNA. Most mutant viruses with single-site

mutations in the F protein did not exhibit a significant difference in virus infectivity compared with the control virus (Table 1). However, for F^{N526S} mutant, the number of copies per TCID₅₀ was $1.0 \times 10^5 \pm 0.3 \times 10^5$. Therefore, the F^{N526S} mutant was considered about 10 times less infectious than the control virus ($P < 0.05$). As the BV titre of F^{N526S} decreased by nearly 10-fold, as determined by an end-point dilution assay, the N-glycosylation site N526 of HaF appears to be important for virus production and infectivity.

Removal of N-glycans at some identified N-glycosylation sites results in increased fusogenicity

The baculovirus F protein is responsible for mediating virus–cell fusion in a low-pH-dependent manner (Ijkel *et al.*, 2000). The fusogenic activities of each mutant were evaluated by syncytium formation assays (Fig. 4a). The F^{N526S} mutant displayed a significantly lower fusion activity (66.1 ± 20.0 %, $P < 0.05$) (Fig. 4b), suggesting the importance of N526 for HaF fusogenicity. However, for most of the single-point mutants (F^{N104S}, F^{N104Q}, F^{N293S}, F^{N361Q} and F^{N571S}), the fusion activity increased about twofold compared with that of the control virus. In addition, the site-rescued mutant F^{N361S} with the compensation of N-glycosylation was also much less efficient in inducing syncytium formation (63.5 ± 19.2 %, $P < 0.05$) (Fig. 4b). Thus, mutation of N-glycosylation sites of HaF was considered to have a profound effect on fusogenicity.

Most N-glycans are involved in the intracellular trafficking of HaF protein

N-Glycosylation contributes to proper glycoprotein folding and intracellular trafficking at different levels (Helenius, 1994). The cell-surface expression levels of the F mutants were quantified by an immunofluorescence assay and flow cytometric analyses (Fig. 5a). The cell-surface level of WT HaF was set as 100 %. When the cells were treated with tunicamycin, an inhibitor that blocks the N-glycosylation process, the expression level of the HaF protein was reduced to ~ 24.0 % ($P < 0.01$), demonstrating that N-glycosylation is important for the trafficking and distribution of F protein in insect cells (Fig. 5a). F^{N595S} showed a similar cell-surface expression level (94.5 ± 1.0 %) to that of the control virus. The level of cell-surface expression of F^{N526S} was reduced by ~ 70 % ($P < 0.01$), suggesting that N526 is an important N-glycosylation site for the efficient transport of F proteins to the cell surface. Most of the other mutants, F^{N104S}, F^{N104Q}, F^{N293S} and F^{N571S}, expressed slightly lower levels of ~ 80 % ($P < 0.05$) of cell-surface HaF in the infected cells compared with the WT control. However, N361 was different from the others as mutations at N361, either F^{N361S} (91.7 ± 1.3 %) or F^{N361Q} (108.0 ± 2.5 %), had a limited impact on the cell-surface expression level of HaF.

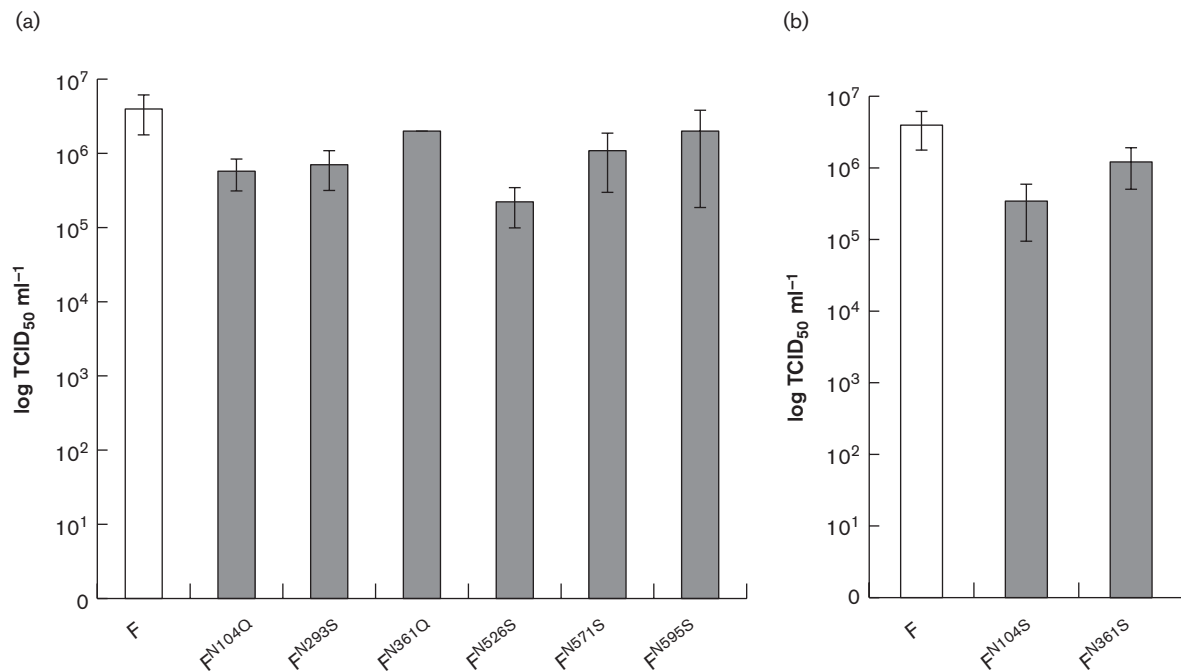


Fig. 3. Analyses of infectious progeny production of mutant viruses. Analysis of infectious BV production of recombinant viruses with mutation at an individual putative *N*-glycosylation site (a) and with created *N*-glycosylation sites (b). BV titres at 72 h p.i. were quantified by an end-point dilution assay. Bars represent the means \pm SD from three independent infections.

The cellular distribution of F protein mutants as the results of mutation of *N*-glycosylation sites was also visualized in *Sf9* cells following fusion with the *egfp* gene (Fig. 5b). When fused with EGFP, WT F protein was located mainly on the cell membrane. For the other mutants, F^{N104S}, F^{N104Q}, F^{N293S} and F^{N571S} appeared in the cytoplasm and at the cell membrane, while F^{N526S} clustered in the cytoplasm (Fig. 5b). These results confirmed that *N*-glycosylation of most sites (N104, N293, N526 and N571) is important for efficient transport of F proteins to the cell surface. F^{N361S} and F^{N361Q} were observed mainly at the cell membrane (Fig. 5b), suggesting a

minor role of *N*-glycans on the rescued N359 or the authentic N361 in F protein transport.

Glycosylation sites are important for F protein folding and transport to the Golgi apparatus

The influence of *N*-glycosylation on HaF folding and trafficking was analysed by a pulse-chase folding assay. The newly synthesized WT F protein was detected as unfolded F₀ at the beginning of the chase (Fig. 6). One other band running slightly faster than the WF F protein was observed under reducing conditions at a chase time

Table 1. Quantitative PCR analysis of BV genomic DNA production and comparison of infectivity of F protein-rescued virus and mutant viruses expressing F proteins with a single mutation

Mutant virus	Genomic DNA (copies ml ⁻¹)	Titre of mutant virus (TCID ₅₀ ml ⁻¹)	Virus infectivity (DNA copies per TCID ₅₀)
vHaBacΔ F-HaF	$8.6 \times 10^{10} \pm 1.7 \times 10^{10}$	$3.5 \times 10^6 \pm 1.5 \times 10^6$	$2.9 \times 10^4 \pm 1.8 \times 10^4$
vHaBacΔ F-F ^{N104S}	$5.6 \times 10^9 \pm 2.8 \times 10^9$	$4.3 \times 10^5 \pm 1.8 \times 10^5$	$1.6 \times 10^4 \pm 1.3 \times 10^4$
vHaBacΔ F-F ^{N104Q}	$6.0 \times 10^9 \pm 0.8 \times 10^9$	$3.7 \times 10^5 \pm 2.3 \times 10^5$	$2.5 \times 10^4 \pm 2.2 \times 10^4$
vHaBacΔ F-F ^{N293S}	$5.5 \times 10^9 \pm 0.2 \times 10^9$	$4.9 \times 10^5 \pm 3.4 \times 10^5$	$1.6 \times 10^4 \pm 1.1 \times 10^4$
vHaBacΔ F-F ^{N361S}	$1.4 \times 10^{10} \pm 0.7 \times 10^{10}$	$5.5 \times 10^5 \pm 2.2 \times 10^5$	$2.7 \times 10^4 \pm 1.1 \times 10^4$
vHaBacΔ F-F ^{N361Q}	$2.1 \times 10^{10} \pm 1.0 \times 10^{10}$	$2.0 \times 10^6 \pm 0.0 \times 10^6$	$1.4 \times 10^4 \pm 0.5 \times 10^4$
vHaBacΔ F-F ^{N526S}	$2.9 \times 10^{10} \pm 0.7 \times 10^{10}$	$2.5 \times 10^5 \pm 0.9 \times 10^5$	$1.0 \times 10^4 \pm 0.3 \times 10^5$
vHaBacΔ F-F ^{N571S}	$1.5 \times 10^{10} \pm 0.6 \times 10^{10}$	$6.0 \times 10^5 \pm 2.9 \times 10^5$	$3.3 \times 10^4 \pm 2.2 \times 10^4$
vHaBacΔ F-F ^{N595S}	$2.8 \times 10^{10} \pm 0.2 \times 10^{10}$	$1.4 \times 10^6 \pm 0.5 \times 10^6$	$2.2 \times 10^4 \pm 0.8 \times 10^4$

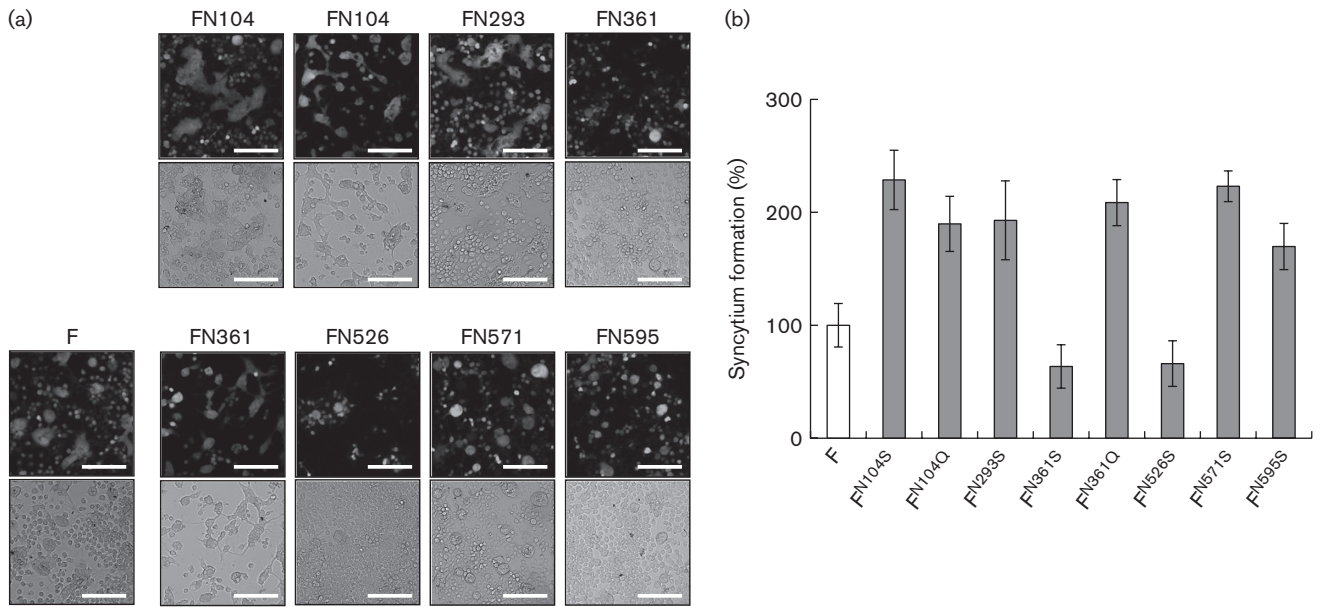


Fig. 4. Syncytium formation assays of HzAM1 cells infected with different mutant viruses. (a) Syncytium formation was observed and images were taken by fluorescence microscopy. Bars, 100 μm. (b) Quantitative characterization of the fusogenic ability of various mutant F proteins. The fusogenic ability of WT HaF protein was set as 100 %. Bars show means ± SD.

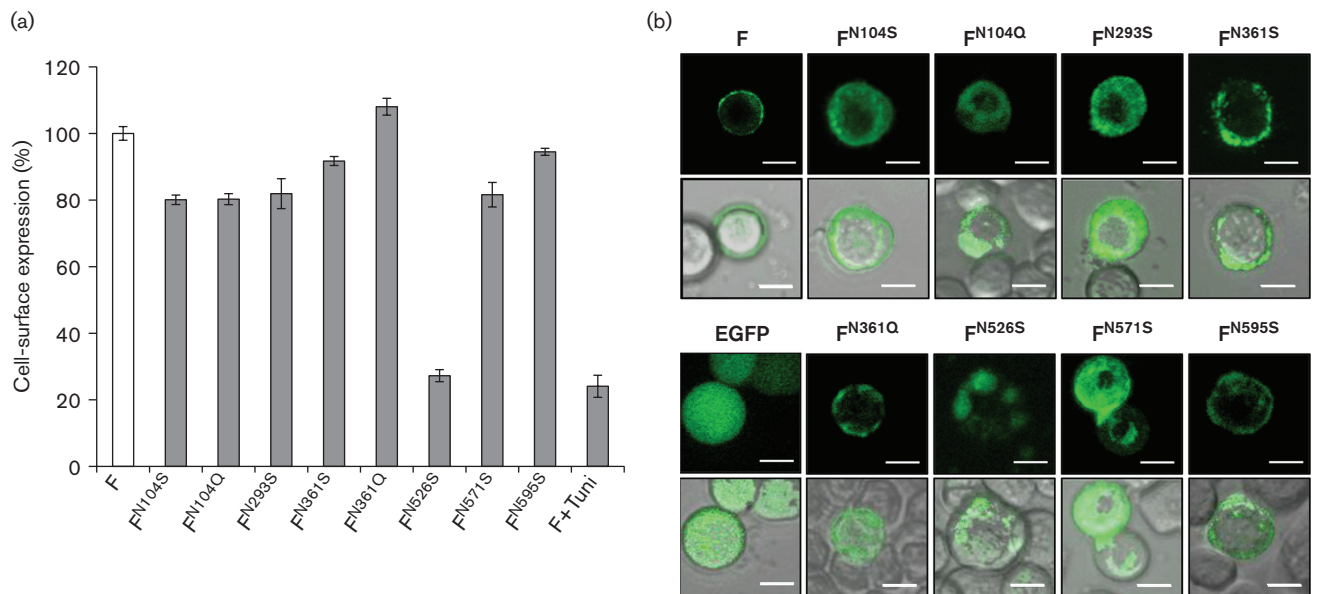


Fig. 5. Determination of the subcellular localization of the different mutant F proteins. (a) Cell-surface levels of mutant or WT F proteins were evaluated by an immunofluorescence assay and flow cytometry. Each sample was tested in triplicate, and bars represent means ± SD. (b) Subcellular localization of WT and mutant F proteins fused with EGFP was visualized in transfected S9 cells. Tuni, tunicamycin. Bars, 10 μm.

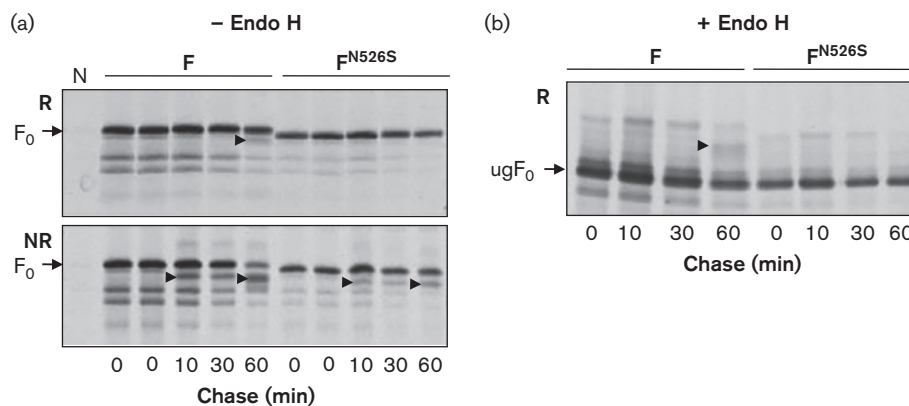


Fig. 6. Folding assay of WT F protein and F^{N526S}. Cells infected with viruses with WT F protein or F^{N526S} were harvested and analysed by a radioactive pulse–chase folding assay. The F proteins were isolated from the detergent cell lysates at the indicated chase times by immunoprecipitation. The F proteins were analysed by 7.5 % SDS-PAGE under reducing (R) and non-reducing (NR) (Lázaro *et al.*, 2007) conditions without treatment with endoglycosidase H (Endo H) (a) and under reducing conditions following treatment with Endo H (b). ugF₀, unglycosylated F₀. Lane N, the healthy cells incubated with anti-F₂ serum as the negative control.

of 60 min (Fig. 6a, upper panel, arrowhead), suggesting that the oligosaccharides of F protein had been processed. The band of lower molecular mass was also detected under non-reducing conditions (Lázaro *et al.*, 2007) at 10 min of chase time (Fig. 6a, bottom panel, arrowhead), indicating that the folding intermediates had already formed by this time. At 60 min of chase, more folding intermediates were detected (Fig. 6a, bottom panel, arrowhead).

As the intracellular transport of F^{N526S} to the cell surface was severely impaired, the folding of F^{N526S} was analysed. No other band of lower molecular mass was observed under reducing conditions until 60 min of chase time (Fig. 6a, upper panel), suggesting that the *N*-linked oligosaccharides of F^{N526S} failed to be processed. In non-reducing conditions (Lázaro *et al.*, 2007), the band of lower molecular mass could be detected after 10 min of chase but less efficiently compared with the WT F protein (Fig. 6a, bottom panel, arrowhead). This result suggested that elimination of the N526 glycosylation site impaired the initial truncation process of *N*-linked oligosaccharides of HaF and decreased the folding efficiency of this protein.

Transfer of the HaF protein from the ER to the Golgi apparatus was investigated using endoglycosidase H (Endo H). Under reducing conditions with Endo H treatment, *N*-glycans of the newly synthesized F protein would be removed to generate unglycosylated F (ugF₀) (Fig. 6b). At 60 min of chase time, a band running slower than ugF₀ was visualized (Fig. 6b, arrowhead), suggesting that a small portion of F protein molecules had been transferred to the Golgi apparatus and that *N*-glycans of the high-mannose type had been processed. However, F^{N526S} was detected only in the ugF₀ form (Fig. 6b), suggesting that F^{N526S} failed to be transported to the Golgi apparatus for

up to 60 min of chase time. These results showed that a mutation at N526 decreased F protein folding efficiency and strongly delayed HaF transport to the Golgi apparatus for further processing.

DISCUSSION

N-Glycosylation is a complex process that first requires the transfer of oligosaccharides onto the potential glycosylation sites in the ER via catalysis of oligosaccharide transferase complex (Burda & Aebi, 1999). Thus, *N*-glycosylation site occupancy is determined at the beginning of the *N*-glycosylation process. However, the site occupancy is not an independent event but relates to several events such as site availability, enzyme kinetics and substrate concentration required for *N*-glycosylation (Jones *et al.*, 2005). Alternatively, not all potential *N*-glycosylation sequons (N-X-S/T) in one glycoprotein molecule will be occupied by *N*-linked oligosaccharides (Jones *et al.*, 2005). In this study, the *N*-glycosylation sites used for HaF protein were mapped precisely. Consistent with the previous report on the *N*-glycoproteomic analysis of HaF NPV BVs where N104, N526 and N571 were found to be glycosylated (Hou *et al.*, 2013), we found that five of the six potential glycosylation sites (N104, N293, N361, N526 and N571) on the HaF protein were *N*-glycosylated, whereas the N595 site was not used. N595 is probably not a used *N*-glycosylation site because it is located in the pre-transmembrane region of F₁ subunit where it may be difficult for the oligosaccharide transferase complex to get access (Fig. 7a). Moreover, the newly created site N102 (in the F^{N104S} mutant) could not fully rescue *N*-glycosylation of the F₂ subunit, suggesting that the unique *N*-glycosylation site N104 in the F₂ subunit may be specific for site occupancy.

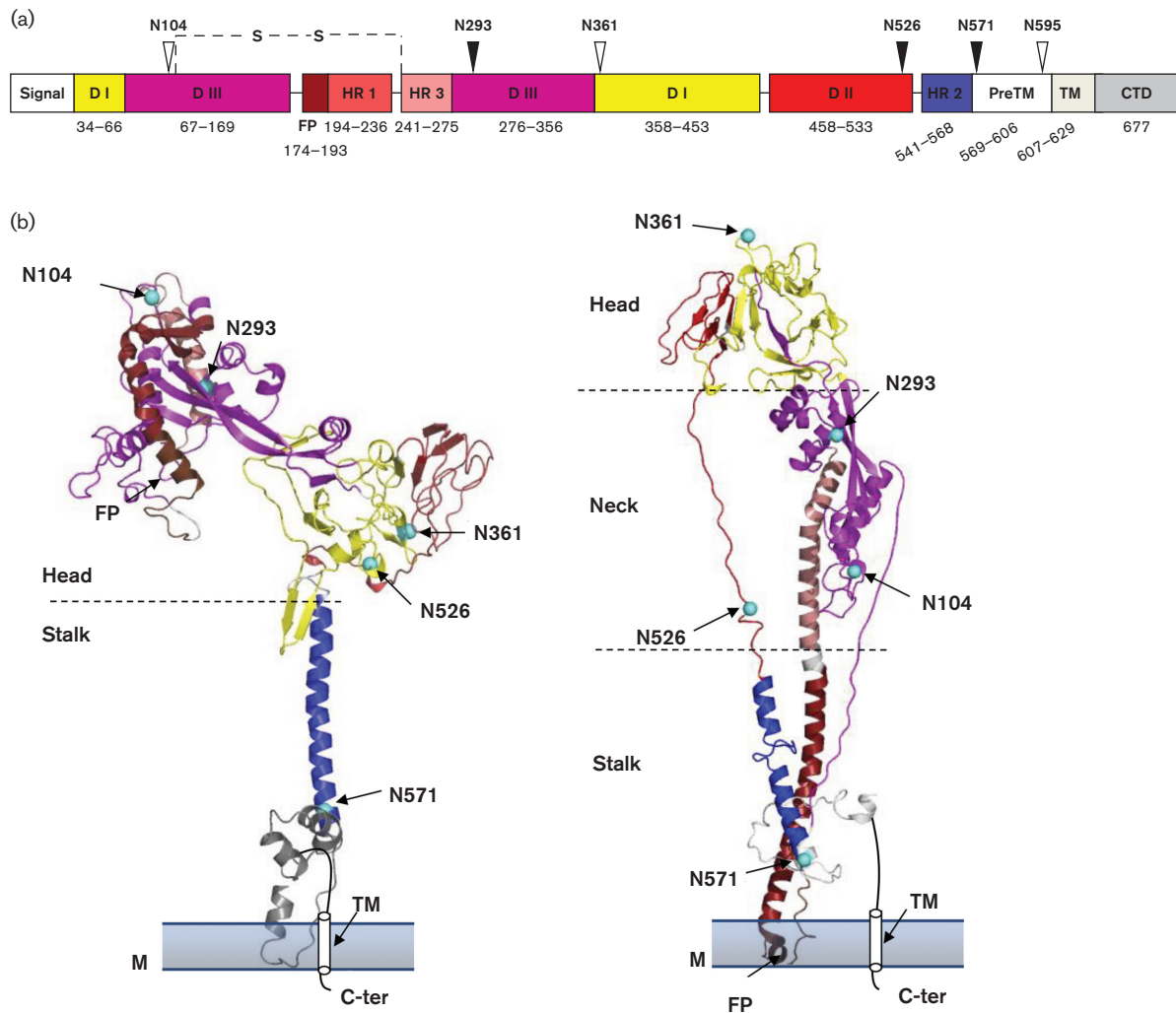


Fig. 7. Computational analysis of *N*-glycosylation sites in primary and tertiary structures of F proteins. (a) Three domains marked with the indicated amino acid positions and different colours were defined in the HaF protein based on alignment with the structural analogues. Predicted *N*-glycosylation sites are indicated by triangles, black ones to conserved sites and white ones to variable sites. The dashed line represents the disulfide bond between the F₁ and F₂ subunits. Signal, signal peptide at the N terminus; D I, domain I; D II, domain II; D III, domain III; FP, fusion peptide; HR, heptad repeat; PreTM, pre-transmembrane region; TM, transmembrane domain; CTD, cytoplasmic tail domain. (b) Cartoon representations of predicted 3D structures of the HaF protein in pre-fusion (left) and post-fusion (right) forms. Domains are colour coded as in (a). The *N*-glycosylation sites used are indicated as cyan spheres. The cylinder near the C terminus (C-ter) represents the transmembrane (TM) region (Bone *et al.*, 1992). M, membrane.

The next step of *N*-glycosylation is that the attached oligosaccharides interact with chaperones, glycosidases and glycosyltransferases in the ER to help protein folding. Only properly folded glycoproteins are transferred to the Golgi apparatus for extensive modification of *N*-glycans (trimming, branching and elongation) after which they are transported to the final destinations inside and outside cells (Burda & Aepli, 1999). Therefore, specific site occupancy of *N*-glycosylation will determine the destiny and property of glycoproteins and thus the protein functioning. Thus, the *N*-glycosylation sites used should be responsible for cellular distribution, trafficking and fusogenicity of HaF

proteins, and consequently affect virus production and infectivity. In general, N526 is a very important *N*-glycosylation site for HaF functions. Other used *N*-glycosylation sites exhibited different degrees of effects on F protein function. As folding assays revealed that F^{N526S} resulted in a decreased efficiency of F protein folding and trafficking, this indicated that mutation of N526 may dramatically change the F protein structure. This may also explain why the fusogenic activity of F^{N526S} was impaired and the amount of infectious progeny viruses and the infectivity of vHaBacΔF-F^{N526S} were decreased significantly. In addition, N361 had limited effects on HaF protein

trafficking, because mutation of N361 did not significantly change the intracellular distribution of F protein. *N*-Linked oligosaccharides attached to conserved asparagine probably play more important roles in ER chaperone recognition and association, and thus are important for glycoprotein folding and trafficking (Jones *et al.*, 2005). Alignment of baculovirus F proteins with putative *N*-glycosylation sites showed that N361 is a unique site of HaF present in a variable region compared with the others (Figs 1a and S2). Therefore, *N*-glycans on N361 may not be essential for HaF folding and trafficking. We also found that most mutant HaF proteins showed enhanced fusogenicity. The data suggested that *N*-glycans except for those on N526 may hinder the fusion process induced by F protein. Further evidence comes from the comparison of increased fusogenicity of F^{N361Q} in which the *N*-glycosylation at N361 is removed, and the decreased fusogenicity of F^{N361S}, which allowed rescue of the *N*-glycosylation of a newly formed sequon at N359.

The roles of *N*-glycosylation have been characterized in evolutionary processes (Gagneux & Varki, 1999; Varki, 2006; Zhang *et al.*, 2004). *N*-Glycosylation events in both hosts and pathogens are determined by mutual selection pressure, and Darwinian selection has been introduced to illustrate the role of *N*-glycosylation sequons in eukaryotes and viruses (Cui *et al.*, 2009). New *N*-glycosylation sites may be developed in virus envelope proteins at 'better' positions (Zhang *et al.*, 2004). Some *N*-glycosylation sites may have been introduced at the expense of certain enhanced properties such as fusogenicity and in exchange for improvement of other function(s) such as virus spread in the environment (Aguilar *et al.*, 2006). We found that, except for N526, *N*-glycans on most sites impaired HaF fusogenicity, an essential trait for virus infection. However, virus production and infectivity of mutant viruses with these mutations were lower than the control virus. This may indicate that the virus traded off higher fusogenic ability for virulence.

The three-dimensional (3D) structures of the F protein of both pre- and post-fusion forms were modelled using the paramyxovirus F proteins as the functional analogue (Chen *et al.*, 2001) (Fig. 7b). Three domains of HearNPV F protein were defined and mapped in the modelled structures as well as the *N*-glycosylation sites (Fig. 7b). The structure of the pre-fusion form is composed of a head (N104, N293, N361 and N526) and a stalk region (N571) (Fig. 7b, left). The post-fusion form was defined with head (N361), neck (N104, N293 and N526) and stalk (N571) regions (Fig. 7b, right). The steric locations of *N*-glycosylation sites of the HaF protein present properties consistent with those of paramyxovirus F proteins (von Messling & Cattaneo, 2003). In general, firstly, in the post-fusion form, the neck region of HaF contains most of the used *N*-glycosylation sites (N104, N293 and N526); secondly, *N*-glycosylation sites involved in efficient intracellular trafficking and folding (N104, N293, N526 and N571) are located in the neck and stalk regions; and thirdly, at least one *N*-glycosylation site (N526) is important for F protein trafficking and folding.

In summary, the *N*-glycosylations in the HearNPV F protein were found to be specific and significant for intracellular transport and egress of the HaF protein and for the fusion activity with host cells. Among the four identified *N*-glycosylation sites on the F₁ subunit, N526 was found to play important roles in both F function and virus infectivity, and N361 is a special site that is not involved in HaF cellular trafficking. Other sites had impacts to various degrees on different properties of the F protein such as intracellular trafficking and fusogenicity. Detailed investigation of how *N*-glycosylation influences baculovirus F protein structure will be of great significance in understanding the functioning of this protein in baculovirus infection and pathogenicity.

METHODS

Insect cells and viruses. *Heliothis zea* HzAM1 cells were cultured at 27 °C in Grace's insect medium (Gibco-BRL) at pH 6.0, supplemented with 10 % (v/v) FBS. The *f*-null bacmid (HaBacΔF) used as a basis for generating glycosylation mutants and the HaF-rescued *f*-null virus (vHaBacΔF-HaF) used as a positive control were generated as described previously (Wang *et al.*, 2008).

Construction of mutant viruses carrying F proteins mutated at all canonical *N*-glycosylation sites. Site-directed mutagenesis was carried out at canonical *N*-glycosylation sites of the HearNPV F protein separately (Fig. 1b). Mutagenic primers (Table S1) were designed so that the asparagine (N)-encoding codon in each *N*-glycosylation sequon (N-X-S/T) was replaced with serine (S)- or glutamine (Q)-encoding codons. Mutant *f*genes were generated using overlap-extension PCR as described (Ho *et al.*, 1989). Mutants carrying single substitutions were designated F^{N104S}, F^{N104Q}, F^{N293S}, F^{N361S}, F^{N361Q}, F^{N526S}, F^{N571S} and F^{N595S}.

PCR products were cloned into pGEM-T Easy vector (Promega), verified by sequencing and then inserted into pFB-Op166 (Wang *et al.*, 2008) using *Eco*RI and *Hind*III restriction sites to generate the transfer plasmids. Each individual plasmid was then transformed into competent DH10Bac cells containing a HaBacΔF bacmid and a helper plasmid expressing a transposase (Bac-to-Bac Baculovirus Expression System; Invitrogen). Mutant bacmids were selected by gentamicin resistance and blue/white screening and identified by PCR with M13 primers.

HzAM1 cells were seeded into 35 mm diameter tissue culture dishes at a density of 3×10^5 cells per dish. After 24 h incubation at 27 °C, cells were transfected with 1 µg bacmid DNA using 12 µl Lipofectin (Invitrogen). At 6 days post-transfection (p.t.), 1 ml supernatant from each transfection was clarified by centrifugation (5 min at 2200 g) and used to infect fresh cells. EGFP expression and spread were determined by fluorescence microscopy.

Western blot analysis of F proteins in mutant BVs and infected cells. BVs were purified from supernatants as described previously (Wang *et al.*, 2008). BVs and infected cells were disrupted by Laemmli sample buffer [125 mM Tris/HCl (pH 6.8), 2 % SDS, 5 % 2-mercaptoethanol, 10 % glycerol, 0.001 % bromophenol blue] and separated by 12 % SDS-PAGE. The proteins in the gel were immobilized on a PVDF membrane and analysed using polyclonal antibodies against F₁ and F₂ (Long *et al.*, 2006) and VP80 (Deng *et al.*, 2007) as primary antibodies, and alkaline phosphatase-conjugated goat anti-rabbit IgG as the secondary antibody (NovoGene Biosciences). Signals were detected with nitro-blue tetrazolium/BCIP (Sino-American Biotechnology Co.).

One-step virus growth curve analysis. One-step virus growth curve analysis was performed as described previously (Wang *et al.*, 2008) with a slight modification. HzAM1 cells (5×10^4 cells per well) were infected at an m.o.i. of 5. Supernatants were harvested at 0, 24, 48, 72 and 96 h p.i. and titrated by an end-point dilution assay. Each virus infection was performed in triplicate. The mean log-transformed TCID₅₀ values and SD were determined using Microsoft Excel Software (version 2003). Significant differences (*P* values) were analysed with one-way ANOVA (Hewson *et al.*, 2004).

Quantitative PCR determination of mutant BV genome copies. Virus infectivity was measured by determining the number of genomic DNA copies compared with viral titres using quantitative PCR with Eva Green dye (Biotium). Viral genomic DNA was purified and used for quantitative PCR analysis as described previously (Wang *et al.*, 2010).

Low-pH-induced envelope fusion assay. A syncytium formation assay was performed as described previously, with slight modifications (Blissard & Wenz, 1992). HzAM1 cells were infected with mutant viruses at an m.o.i. of 5. At 48 h p.i., the cells were rinsed three times with Grace's insect medium (pH 6.0) and treated with 1 ml acidic Grace's insect medium (pH 4.8) for 5 min. The cells were then further cultured with Grace's insect medium containing 10 % FBS at a normal pH (pH 6.0) for 24 h followed by fluorescence microscopy.

The cells were fixed, washed and incubated with Hoechst 33258 (Biotium) for 15 min at room temperature. After three washes, the cells were photographed. The fusion ability of BVs containing WT and mutant F proteins was measured as described elsewhere, with slight modifications (Long *et al.*, 2007; Tan *et al.*, 2008). Syncytial masses were defined as fused cells containing four or more nuclei. Five fields were chosen randomly for each analysis. The fusogenic ability was calculated as the number of fused cells compared with infected cells. The mean value of the fusogenic ability of WT F protein was set as 100 %.

Subcellular localization of mutant HaF proteins. To determine the localization of different mutant F proteins in insect cells, p166AcV5-*fx-egfp* plasmids (*fx* represents WT or mutant *f* genes) were constructed, allowing the expression of fused EGFP at the C terminus of F proteins in insect cells. The stop codons were deleted from the parental and mutant *f* genes when they were PCR amplified with primers HaFdelTAAfor and HaFdelTAArev (Table S1) and verified by sequencing. Subsequently, the fragments were cloned into the p166AcV5-*egfp* plasmid (IJkel *et al.*, 2000) at the *Hind*III restriction site in frame with the *egfp* gene. Sf9 cells (1×10^6 cells per well) were transfected with the plasmids and examined in a Leica S2 confocal laser scanning fluorescence microscope at 48 h p.i.

The cell-surface levels of mutant HaF proteins were analysed quantitatively by an immunofluorescence assay and flow cytometry analysis (Tong *et al.*, 2001). HzAm1 cells were infected with viruses at an m.o.i. of 5. At 24 h p.i. the cells were rinsed twice with PBS and blocked for 1 h at 27 °C with PBS containing 5 % BSA. The cells were then incubated with anti-F₂ antiserum (1 : 500 dilution) overnight at 4 °C and with a secondary goat anti-rabbit antibody conjugated with R-phycoerythrin (1 : 300 dilution; Proteintech Group) for 1 h at 27 °C. The cells were washed and resuspended for flow cytometry analysis on a Beckman Coulter EPICS XL flow cytometer. Infected cells expressing EGFP and immunostained with R-phycoerythrin were scored. The relative levels of F proteins on the cell surface were measured by dividing the percentage of cells stained with R-phycoerythrin by the number expressing EGFP, and these levels were normalized to the data from the WT control, which was set as 100 %.

Protein folding assays. F protein folding was investigated using pulse-chase experiments performed essentially as described previously (Braakman & Hebert, 2001; Braakman *et al.*, 1991; Land *et al.*, 2003).

HzAM1 cells were infected with viruses at an m.o.i. of 5. Cells were harvested at 48 h p.i. and depleted of methionine for 15–30 min before they were pulse labelled with pro-mix [³⁵S]cysteine and [³⁵S]methionine (Easytag Express Protein Labelling Mix; PerkinElmer). Cells were chased for various intervals in medium containing an excess of unlabelled methionine. Chase samples were stopped by aspirating the medium and adding ice-cold Hanks' balanced salt solution (Invitrogen-BRL) containing 20 mM N-ethylmaleimide to block free thiol groups. Cells were lysed in ice-cold 0.5 % (v/v) Triton X-100 in MNT [20 mM MES (pH 7.5), 100 mM NaCl, 30 mM Tris/HCl] and protease inhibitor cocktail (10 µg ml⁻¹ each chymostatin, leupeptin, antipain, and pepstatin, 1 mM PMSF and 1 mM EDTA). Cell lysates were spun for 10 min at 15 000 g at 4 °C to sediment the nuclei.

Immunoprecipitation was used to isolate the F proteins. Goat anti-rabbit IgG (1 µg per sample) was incubated for 1 h at 4 °C with protein A-Sepharose 4B fast-flow beads (50 µl 10 % suspension per sample; Amersham Pharmacia Biotech AB). Anti-F₂ serum used as the primary antibody was added, and incubation was continued for 1 h. Cell lysates were added to the mixture and incubated at 4 °C for 1 h. The immunoprecipitates were washed twice for 10 min each with wash buffer [10 mM Tris/HCl (pH 8.6), 0.05 % Triton X-100, 0.1 % SDS, 0.3 M NaCl] at room temperature; the washed pellets were resuspended in 20 µl 10 mM Tris/HCl (pH 6.8) and sample buffer was added to a final concentration of 200 mM Tris/HCl (pH 6.8), 3 % SDS, 10 % glycerol, 0.004 % bromophenol blue and 1 mM EDTA. Samples were incubated at 95 °C for 5 min and analysed by reducing or non-reducing 7.5 % SDS-PAGE (Braakman *et al.*, 1991). The gels were then dried and signals were detected on Biomax MR films (Eastman Kodak).

For Endo H digestion, immunoprecipitates were resuspended in 0.2 % SDS in 100 mM sodium acetate (pH 5.5) and heated for 5 min at 95 °C. An equal volume of 100 mM sodium acetate (pH 5.5) was then added. Endo H (0.2 U) (Scalia *et al.*, 1992) was added to each sample and incubated for 1 h at 37 °C.

Computational analysis of putative N-glycosylation sites and their superposition on the constructed 3D structure of HaF.

Sequences of F proteins of group II alphabaculoviruses were aligned using MEGALIGN in DNASTAR and edited with Genedoc software. Putative N-glycosylation sites of the F proteins were predicted with the NetNGlyc 1.0 Server (ExPASy, Swiss Institute of Bioinformatics). The Phyre threading program (<http://www.sbg.bio.ic.ac.uk/~phyre>) was used to search appropriate templates for 3D computer animation. Simian virus 5 (SV5) F protein (PDB code: 2b9b) was used as the template for the pre-fusion state of HaF. Sequence alignment with HaF and SV5 F protein was carried out using CLUSTALW version 2.0 (<http://www.ebi.ac.uk/Tools/msa/clustalw2/>) and the 3D structure was modelled in the alignment mode of SWISS-MODEL (Arnold *et al.*, 2006; Kiefer *et al.*, 2009; Peitsch, 1995). The post-fusion structure was modelled by i-TASSER (Roy *et al.*, 2010), and is a structure analogue compared with the human parainfluenza virus type 3 (HPIV3) F protein (PDB code: 1ZTM). Domains of the HaF protein were defined according to those of SV5 F and HPIV3 F proteins by using William Pearson's LALIGN program as described elsewhere (Garry & Garry, 2008). The 3D structures were displayed using Pymol version 0.99.

ACKNOWLEDGEMENTS

This work was supported by the National Natural Science Funds for Distinguished Young Scholars (grant no. 31125003), the Strategic Priority Research Program of the Chinese Academy of Sciences (grant no. XDB11030400), the National Natural Science Foundation

of China (grant nos 31100120 and 31370191), and a PSA project from the Ministry of Science and Technology of China and the Royal Academy of Sciences of the Netherlands (grant no. 2008DFB30220 to China and no. 08-PSA-BD-01 to the Netherlands). We acknowledge the Core Facility and Technical Support of Wuhan Institute of Virology for technical assistance.

REFERENCES

- Abe, Y., Takashita, E., Sugawara, K., Matsuzaki, Y., Muraki, Y. & Hongo, S. (2004). Effect of the addition of oligosaccharides on the biological activities and antigenicity of influenza A/H3N2 virus hemagglutinin. *J Virol* **78**, 9605–9611.
- Aguilar, H. C., Matreyek, K. A., Filone, C. M., Hashimi, S. T., Levrony, E. L., Negrete, O. A., Bertolotti-Ciarlet, A., Choi, D. Y., McHardy, I. & other authors (2006). N-glycans on Nipah virus fusion protein protect against neutralization but reduce membrane fusion and viral entry. *J Virol* **80**, 4878–4889.
- Arnold, K., Bordoli, L., Kopp, J. & Schwede, T. (2006). The SWISS-MODEL workspace: a web-based environment for protein structure homology modelling. *Bioinformatics* **22**, 195–201.
- Blissard, G. W. & Wenz, J. R. (1992). Baculovirus gp64 envelope glycoprotein is sufficient to mediate pH-dependent membrane fusion. *J Virol* **66**, 6829–6835.
- Bone, R. C., Balk, R., Slotman, G., Maunder, R., Silverman, H., Hyers, T. M. & Kerstein, M. D. (1992). Adult respiratory distress syndrome. Sequence and importance of development of multiple organ failure. The Prostaglandin E1 Study Group. *Chest* **101**, 320–326.
- Braakman, I. & Hebert, D. N. (2001). Analysis of disulfide bond formation. *Curr Protoc Protein Sci* **3**, 1411–14115.
- Braakman, I., Hoover-Litty, H., Wagner, K. R. & Helenius, A. (1991). Folding of influenza hemagglutinin in the endoplasmic reticulum. *J Cell Biol* **114**, 401–411.
- Burda, P. & Aebi, M. (1999). The dolichol pathway of N-linked glycosylation. *Biochim Biophys Acta* **1426**, 239–257.
- Chen, L., Gorman, J. J., McKimm-Breschkin, J., Lawrence, L. J., Tulloch, P. A., Smith, B. J., Colman, P. M. & Lawrence, M. C. (2001). The structure of the fusion glycoprotein of Newcastle disease virus suggests a novel paradigm for the molecular mechanism of membrane fusion. *Structure* **9**, 255–266.
- Cui, J., Smith, T., Robbins, P. W. & Samuelson, J. (2009). Darwinian selection for sites of Asn-linked glycosylation in phylogenetically disparate eukaryotes and viruses. *Proc Natl Acad Sci U S A* **106**, 13421–13426.
- Danielsson, R., Bååth, M., Kölbeck, K. G., Klominek, J. & Svensson, L. (2003). Accumulation of Tc-99m depreotide (NeoSpect) in axillary sweat glands. *Clin Nucl Med* **28**, 789–790.
- Deng, F., Wang, R., Fang, M., Jiang, Y., Xu, X., Wang, H., Chen, X., Arif, B. M., Guo, L. & other authors (2007). Proteomics analysis of *Helicoverpa armigera* single nucleocapsid nucleopolyhedrovirus identified two new occlusion-derived virus-associated proteins, HA44 and HA100. *J Virol* **81**, 9377–9385.
- Gagneux, P. & Varki, A. (1999). Evolutionary considerations in relating oligosaccharide diversity to biological function. *Glycobiology* **9**, 747–755.
- Garry, C. E. & Garry, R. F. (2008). Proteomics computational analyses suggest that baculovirus GP64 superfamily proteins are class III penitrenes. *Virology* **5**, 28.
- Helenius, A. (1994). How N-linked oligosaccharides affect glycoprotein folding in the endoplasmic reticulum. *Mol Biol Cell* **5**, 253–265.
- Hewson, R., Gmyl, A., Gmyl, L., Smirnova, S. E., Karganova, G., Jamil, B., Hasan, R., Chamberlain, J. & Clegg, C. (2004). Evidence of segment reassortment in Crimean-Congo haemorrhagic fever virus. *J Gen Virol* **85**, 3059–3070.
- Ho, S. N., Hunt, H. D., Horton, R. M., Pullen, J. K. & Pease, L. R. (1989). Site-directed mutagenesis by overlap extension using the polymerase chain reaction. *Gene* **77**, 51–59.
- Hou, D., Zhang, L., Deng, F., Fang, W., Wang, R., Liu, X., Guo, L., Rayner, S., Chen, X. & other authors (2013). Comparative proteomics reveal fundamental structural and functional differences between the two progeny phenotypes of a baculovirus. *J Virol* **87**, 829–839.
- IJkel, W. F., Westenberg, M., Goldbach, R. W., Blissard, G. W., Vlak, J. M. & Zuidema, D. (2000). A novel baculovirus envelope fusion protein with a proprotein convertase cleavage site. *Virology* **275**, 30–41.
- Jones, J., Krag, S. S. & Betenbaugh, M. J. (2005). Controlling N-linked glycan site occupancy. *Biochim Biophys Acta* **1726**, 121–137.
- Kadlec, J., Loureiro, S., Abrescia, N. G., Stuart, D. I. & Jones, I. M. (2008). The postfusion structure of baculovirus gp64 supports a unified view of viral fusion machines. *Nat Struct Mol Biol* **15**, 1024–1030.
- Kiefer, F., Arnold, K., Künzli, M., Bordoli, L. & Schwede, T. (2009). The SWISS-MODEL repository and associated resources. *Nucleic Acids Res* **37** (Database issue), D387–D392.
- Land, A., Zonneveld, D. & Braakman, I. (2003). Folding of HIV-1 envelope glycoprotein involves extensive isomerization of disulfide bonds and conformation-dependent leader peptide cleavage. *FASEB J* **17**, 1058–1067.
- Lázaro, M. E., Cantoni, G. E., Calanni, L. M., Resa, A. J., Herrero, E. R., Iacono, M. A., Enria, D. A. & González Cappa, S. M. (2007). Clusters of hantavirus infection, southern Argentina. *Emerg Infect Dis* **13**, 104–110.
- Long, G., Westenberg, M., Wang, H., Vlak, J. M. & Hu, Z. (2006). Function, oligomerization and N-linked glycosylation of the *Helicoverpa armigera* single nucleopolyhedrovirus envelope fusion protein. *J Gen Virol* **87**, 839–846.
- Long, G., Pan, X. & Vlak, J. M. (2007). Absence of N-linked glycans from the F2 subunit of the major baculovirus envelope fusion protein F enhances fusogenicity. *J Gen Virol* **88**, 441–449.
- Ohuchi, M., Ohuchi, R., Feldmann, A. & Klenk, H. D. (1997a). Regulation of receptor binding affinity of influenza virus hemagglutinin by its carbohydrate moiety. *J Virol* **71**, 8377–8384.
- Ohuchi, R., Ohuchi, M., Garten, W. & Klenk, H. D. (1997b). Oligosaccharides in the stem region maintain the influenza virus hemagglutinin in the metastable form required for fusion activity. *J Virol* **71**, 3719–3725.
- Pearson, M. N., Groten, C. & Rohrmann, G. F. (2000). Identification of the *Lymantria dispar* nucleopolyhedrovirus envelope fusion protein provides evidence for a phylogenetic division of the *Baculoviridae*. *J Virol* **74**, 6126–6131.
- Peitsch, M. C. (1995). Protein modeling by e-mail. *Biotechnology (N Y)* **13**, 658–660.
- Roy, A., Kucukural, A. & Zhang, Y. (2010). I-TASSER: A unified platform for automated protein structure and function prediction. *Nat Protoc* **5**, 725–738.
- Scalia, S., Sharma, P., Rodriguez, J., Roche, F., Luchette, F., Chambers, R., Flint, L. M. & Steinberg, S. (1992). Decreased mesenteric blood flow in experimental multiple organ failure. *J Surg Res* **52**, 1–5.
- Tan, Y., Jiang, L., Wang, M., Yin, F., Deng, F., Liu, M., Hu, Z. & Wang, H. (2008). Mutagenesis and nuclear magnetic resonance analyses of the fusion peptide of *Helicoverpa armigera* single nucleocapsid nucleopolyhedrovirus F protein. *J Virol* **82**, 8138–8148.

- Tong, S., Yi, F., Martin, A., Yao, Q., Li, M. & Compans, R. W. (2001).** Three membrane-proximal amino acids in the human parainfluenza type 2 (HPIV 2) F protein are critical for fusogenic activity. *Virology* **280**, 52–61.
- Varki, A. (2006).** Nothing in glycobiology makes sense, except in the light of evolution. *Cell* **126**, 841–845.
- von Messling, V. & Cattaneo, R. (2003).** N-linked glycans with similar location in the fusion protein head modulate paramyxovirus fusion. *J Virol* **77**, 10202–10212.
- Wang, M., Tan, Y., Yin, F., Deng, F., Vlak, J. M., Hu, Z. & Wang, H. (2008).** The F protein of *Helicoverpa armigera* single nucleopolyhedrovirus can be substituted functionally with its homologue from *Spodoptera exigua* multiple nucleopolyhedrovirus. *J Gen Virol* **89**, 791–798.
- Wang, M., Yin, F., Shen, S., Tan, Y., Deng, F., Vlak, J. M., Hu, Z. & Wang, H. (2010).** Partial functional rescue of *Helicoverpa armigera* single nucleocapsid nucleopolyhedrovirus infectivity by replacement of F protein with GP64 from *Autographa californica* multicapsid nucleopolyhedrovirus. *J Virol* **84**, 11505–11514.
- Westenberg, M., Veenman, F., Roode, E. C., Goldbach, R. W., Vlak, J. M. & Zuidema, D. (2004).** Functional analysis of the putative fusion domain of the baculovirus envelope fusion protein F. *J Virol* **78**, 6946–6954.
- Zhang, M., Gaschen, B., Blay, W., Foley, B., Haigwood, N., Kuiken, C. & Korber, B. (2004).** Tracking global patterns of N-linked glycosylation site variation in highly variable viral glycoproteins: HIV, SIV, and HCV envelopes and influenza hemagglutinin. *Glycobiology* **14**, 1229–1246.